

Three-dimensional Evolution of the Polar Vortex during the New Year's 1994 Stratospheric Warming

G. I. Manney, R. W. Zurek,
Jet Propulsion Laboratory/California Institute of Technology, Pasadena USA

R. Swinbank,
Meteorological Office, Bracknell UK

Received _____; accepted _____

Submitted to *Geophysical Research Letters*, March 1995.

Short title: NEWYEAR'S 1994 STRATOSPHERIC WARMING

Abstract. High-resolution trajectory calculations are used to show the patterns of the circulation as a function of height during a strong stratospheric warming in early Jan 1994. In the middle and upper stratosphere, where there is a closed anticyclonic circulation, material drawn off the vortex and material drawn in from low latitudes coil up together in the anticyclone; the amount of material from the vortex that is included increases with height. In the lower stratosphere, where there is no closed anticyclonic circulation, the extra-vortex flow is characterized by folding and stretching of narrow filaments that are drawn in from low latitudes and off the vortex. At levels where the closed anticyclonic circulation organizes the extra-vortex flow, parcels in the anticyclone descend farthest during the warming; at lower levels, parcels near the vortex edge descend most.

Introduction

Stratospheric warmings have a profound effect on the evolution of the polar vortex during the NH winter. The United Kingdom Meteorological Office (UKMO) developed a data assimilation system in support of the Upper Atmosphere Research Satellite (UARS) program [Swinbank and O'Neill 1994], which provides a quality controlled meteorological dataset with good spatial resolution in the stratosphere, and wind fields that are consistent with the primitive equations used for the general circulation model into which observations are assimilated. It has been demonstrated [e.g., O'Neill *et al.* 1994] that these analyses are a powerful tool for studying stratospheric warmings and the evolution of the stratospheric circulation.

O'Neill *et al.* [1994] used the UKMO analyses, and “domain-filling” trajectory calculations on isentropic surfaces using UKMO winds to describe in detail the evolution of the stratospheric flow during a strong warming in late January 1992. We examine here, in a similar manner, the three-dimensional evolution of the circulation in and around the polar vortex during a strong stratospheric warming near the beginning of 1994. Three-dimensional domain-filling trajectory calculations are used to describe in detail the patterns of diabatic descent during this event, and the variations in these patterns with height.

Data and Analysis

The UKMO data assimilation system is described by Swinbank and O'Neill [1994]; geopotential heights, temperatures and horizontal winds are provided on levels equally spaced in $\log(\text{pressure})$, with six levels per decade in pressure throughout the stratosphere. Rossby-Ertel potential vorticity (PV) is calculated from the UKMO analyses; for vertical sections, PV is scaled in “vorticity units” (s^{-1}) [e.g., Manney *et al.*, 1994a] to give a similar range of values at all levels.

The trajectory code [Manney *et al.* 1994a] uses UKMO horizontal winds and, because radiative heating rates from the UKMO assimilation model are not available as an output product, diabatic descent rates from an independent radiation code, MILDAD, a recent version of the code described by Shine [1987]. Nearly 60,000 parcels have been initialized on an equal area grid covering the NH on 6 isentropic surfaces covering the stratosphere. As was done by O'Neill *et al.* [1994], the parcels are color coded by their PV on the initial day, providing a high resolution picture of the evolution of the flow on succeeding days. In addition, we examine the motion of the parcels with respect to isentropic surfaces to get a detailed picture of the three-dimensional patterns of diabatic descent.

Results

Fig. 1 shows time series from 16 Dec 1993 through 14 Jan 1994 of 10 hPa zonal mean wind and temperature. A reversal of high latitude winds and temperature gradients occurs in the last few days of December and the first few days of January, with the peak of the warming around 1 Jan 1994. The wind reversal is in the region north of $\approx 64^\circ\text{N}$. As will be seen below, this event resembled what is sometimes called a “wave 2” warming, where the mid-stratospheric vortex is elongated and split, or nearly split, into two lobes. During this warming, lower stratospheric temperatures rose above the threshold for polar stratospheric cloud formation [Waters *et al.* 1995], and, while the circulation in the middle and upper stratosphere recovered shortly after this event, the lower stratospheric vortex was substantially weakened and remained weak until a brief strengthening in late February 1994 [Manney *et al.* 1995].

The large-scale vertical structure of the polar vortex during the warming is shown in Fig. 2, a few days before (27 Dec 1993) and a few days after (4 Jan 1994) the peak of the warming. Scaled PV and heating rates calculated by MILDAD are shown as a function of latitude along 45° to 255°E , and as a function of longitude around

60°N. The pattern of temperatures closely follows that of the heating rates shown here, with highest temperatures coincident with regions of strongest diabatic descent. The strongest diabatic descent is along the region of strong PV gradients in the upper stratosphere; in the middle and lower stratosphere, most enhanced cooling is seen in the region of the anticyclone, outside the region of strong PV gradients.

Although this warming is not as strong, the general evolution of the vertical structure of the flow strongly resembles that shown by *Manney et al. [1994b]* for simulations of the February 1979 stratospheric warming. A baroclinic zone forms in the temperature (and heating) field before the peak of the warming, with the vortex tilting westward (Fig. 2c) and outward (Fig. 2a) with increasing height. As the warming progresses, the vortex straightens up, so that after the peak the vortex shows no tilt with latitude (Fig. 2b) and less tilt with longitude (Fig. 2d).

Figure 3 shows high-resolution PV fields from the don-lain-filling trajectory calculations initialized on 25 Dec 1993, for parcels initialized at 840 K, throughout the warming. By 30 Dec, the anticyclone has already strengthened, and a tongue of high-PV material is pulled off the vortex, and wrapped partially around the anticyclone. Over the course of the warming, low PV air is drawn up from low latitudes and coiled up into the anticyclone with high PV material drawn off the vortex. Most of the low latitude air is drawn in between the cyclone and anticyclone; however, some low PV air is also drawn in directly from around the southern side of the anticyclone (e.g., 30 Dec, 3 Jan). The low latitude air thus arrives in the anticyclone by different paths, with the possibility of very different sun exposure and thermal history. Both the stripping of vortex air and the drawing in of subtropical air will sharpen tracer gradients along the vortex edge. Similar coiling of material in the anticyclone was noted during the late January 1992 warming [*O'Neill et al. 1994*], and led to rippled features in observed tracer fields [*Lahoz et al. 1994*]. Additional folding and stretching occurs in the region where air is drawn between the vortex and the anticyclone (e. g., near 130°E, 40° N on

30 Dec, 3 Jan and 5 Jan and where material is drawn off the vortex (e.g., near 240°E, 40°N on 3 Jan).

On 1 Jan, the vortex is at its maximum elongation at 840 K, and is nearly split. The development of closed vortices in each lobe removes high PV material from the region between them by wrapping it into the vortices. On the succeeding days, the smaller western vortex weakens and its material is pulled back into and sheared out around the stronger eastern vortex. During this process, relatively low PV material from the vortex edge region between the lobes is wrapped into the expanding eastern vortex. By 5 Jan, this material can be seen well within the interior of the region of very high PV . These vortex interactions are particularly effective at mixing vortex air and entraining vortex-edge and extra-vortex air deep within the polar vortex. If the vortex air were originally radially stratified within the vortex, as may result from descent of mesospheric air [Fisher *et al.* 1993], such stratification would be lost during warmings as strong as this one.

Fig. 4 shows the evolution of the flow on the same days, but for parcels initialized at 420 K, near the bottom of the stratosphere. At this level, there is no closed anticyclonic circulation, and instead of the stripping off of high- PV tongues which become progressively narrower and roll up with the low- PV tongues drawn in from low latitudes, the appearance of the flow in the extra-vortex region is characterized by stretching and folding of narrow filaments of low- PV air from low latitudes, and high- PV air drawn off the vortex. This behavior is seen throughout the mid-latitude extra-vortex region, not just underlying the anticyclone.

As at higher levels, the lower stratospheric vortex is pulled out into two main lobes on 1 Jan, and by 3 Jan the smaller sub-vortex begins to be drawn in and sheared out around the larger. However, by 5 Jan, the larger vortex is itself drawn out into two sub-vortices. We thus see at these levels a continuing process of vortex development where sub-vortices form and then merge, as the weaker ones are sheared out around

the stronger. Although a polar vortex, in the sense of a region of strong PV gradients resulting from the strong winds in the polar night jet, can be defined at this levels, it is clearly more complicated than the relatively strongly isolated, single vortex that is seen at higher levels.

Fig. 5 illustrates the changes with height in the patterns of vortex evolution, showing on 1 Jan, near the peak of the warming, the domain-filling trajectory calculations for parcels started at 520 K, 655 K, and 1100 K (the parcels started at 420 K for this day were shown in Fig. 4, and those started at 840 K in Fig. 3). At 520 K, the polar vortex already has the relatively simple, “wave 2” structure that was seen at 840 K. However, there is still not a closed anticyclonic circulation at this level, and the extra-vortex behavior is characterized by stretching and folding, rather than the pulling out and coiling up of long tongues that was apparent at 840 K. A closed anticyclone is apparent at 655 K, and the coiling up of material drawn in from low latitudes into the anticyclone is apparent. However, the large tongues of material being drawn off the vortex and around the anticyclone are not as large as at 840 K.

At 1100 K, and at 1300 K (not shown), the vortex is not as divided as at the lower levels, having more of a “wave 1” type structure, with a very large, strong closed anticyclone. The tongues of high PV drawn off the vortex are larger, and considerable amounts of material with both very high and very low PV are coiled up together in the anticyclone. More high PV air is drawn off the vortex and coiled up into the anticyclone than at the lower levels, consistent with the stronger jet between the cyclone and anticyclone.

Fig. 6 shows how the patterns of diabatic descent change through the stratosphere. The potential temperatures of parcels started at 655 K, 520 K, and 420 K are shown on 9 Jan 1994, day 15 of the domain-filling trajectory calculation, after the warming. At 655 K, and all levels above (not shown), where there is a closed anticyclonic circulation, the parcels coiled up in the anticyclone experience considerably more descent than any

others. There is somewhat stronger descent around the edge of the vortex region than in the center. As was seen in Fig. 2, and has been previously noted [e.g. *Manney et al. 1994a*], the strongest diabatic cooling rates are typically in the region between the cyclone and anticyclone, but may at times be well out into the anticyclone in the mid-stratosphere (e.g. Fig. 2b). The parcels that coil up in the anticyclone thus remain in the region of strongest descent rates, and those that circulate around the edge of the vortex pass through regions of stronger descent than those near the center of the vortex.

At the lower levels, both 420 K and 520 K, where there is no closed anticyclonic circulation, the strongest diabatic cooling remains along or outside the vortex edge (Fig. 2). At these levels, the only organized pattern where parcels continuously circulate through the region of strongest descent is around the edge of the vortex. Consistent with this, the parcels along the vortex edge have generally experienced the most descent (Fig. 6b, 6c).

Summary

Meteorological data and domain-filling trajectory calculations reveal details of the evolution of the stratospheric polar vortex during a strong “wave 2” type stratospheric warming in early Jan 1994. Our results show previously noted features, such as the formation of a baroclinic zone in temperature, and the westward and outward tilt of the vortex with height during the early part of the warming. The domain-filling trajectory calculations show changes in the patterns of the circulations with height. In the middle and upper stratosphere, where there is a closed anticyclonic circulation, the material contours are seen to coil up in the anticyclone, rolling up together material drawn off the vortex and material drawn in from low latitudes. The amount of material drawn off the vortex that is included in this coil increases with height, consistent with the stronger vortex anticyclone in the upper stratosphere. In the lower stratosphere, below the level where there is a closed anticyclonic circulation, the extra-vortex circulation is

characterized by folding and stretching of narrow filaments that are drawn in from low latitude and off the vortex. Near-separation of the vortex into sub-vortices and their subsequent merging during the warming results in the entrainment of vortex-edge and extra-vortex air deep into the vortex throughout the lower and middle stratosphere. At the levels where the closed anticyclonic circulation organizes the extra-vortex flow, the parcels that coil up in the anticyclone experience the most descent. At lower levels, the parcels circulating around the vortex edge experience the most descent.

Acknowledgments. We thank I. Luu for data management, P. Newman for supplying the original PV routines. This work was part of a UARS Theoretical Investigation at the Jet Propulsion Laboratory, California Institute of Technology, and was done under contract with the National Aeronautics and Space Administration.

References

- Fisher, M., A. O'Neill, and R. Sutton, Rapid descent of mesospheric air in the stratospheric polar vortex, *Geophys. Res. Lett.*, 20, 1267-1270, 1993.
- Lahoz, W. A., et al., Three-dimensional evolution of water vapour distributions in the Northern Hemisphere stratosphere as observed by MIS, *J. Atmos. Sci.*, 51, 2914- 2930, 1994.
- Manney, G. L., R. W. Zurek, A. O'Neill, and R. Swinbank, on the motion of air through the stratospheric polar vortex, *J. Atmos. Sci.*, 51, 2973-2994, 1994a.
- Manney, G. L., J. D. Farrara, and C. R. Mechoso, Simulations of the February 1979 stratospheric sudden warming: Model comparisons and three-dimensional evolution, *Mon. Weather Rev.*, 122, 1115-1140, 1994b.
- Manney, G. L., L. Froidevaux, J. W. Waters, and R. W. Zurek, Evolution of MIS ozone and the polar vortex during winter, *J. Geophys. Res.*, in press, 1995.
- O'Neill, A., W. L. Grose, V. D. Pope, H. MacLean, and R. Swinbank, Evolution of the stratosphere during northern winter 1991/92 as diagnosed from U.S. Meteorological Office analyses, *J. Atmos. Sci.*, 51, 2800-2817, 1994.
- Shine, K. P., The middle atmosphere in the absence of dynamic heat fluxes, *Q. J. R. Meteorol. Soc.*, 113, 603-633, 1987.
- Swinbank, R., and A. O'Neill, A Stratosphere-troposphere data assimilation system, *Mon. Weather Rev.*, 122, 686-702, 1994.
- Waters, J. W., G. L. Manney, W. G. Read, L. Froidevaux, D. A. Flower, and R. F. Jarnot, UARS MIS observations of lower stratospheric ClO in the 1992-93 and 1993-94 Arctic winter vortices, *Geophys. Res. Lett.*, in press, 1995.

Figure 1. Timeseries of (a) zonal mean wind (m/s) and (b) zonal mean temperature (K) at 10 hPa for 16 Dec 1993 through 14 Jan 1993. Negative values are shaded in (a); shading in (b) is between 255 and 230 K. The horizontal line is across 60°N.

Figure 2. Cross-sections of diabatic heating rates (colors, K/d) and scaled PV (contours, 10^{-4}s^{-1}) on 27 Dec 1993 and 4 Jan 1994, (a) and (b) versus latitude and θ along 45- 255°E, and (c) and (d) versus longitude and θ at 60°N.

Figure 3. Time sequence of the distribution of parcels started on the 840 K isentropic surface, color coded by their PV ($10^{-4}\text{Km}^2\text{kg}^{-1}\text{s}^{-1}$) in the initial day, 25 Dec 1993.

Figure 4. As ~~Fig.~~ ^{Fig.} 3, but for parcels started at 420 K.

Figure 5. As in Fig 3, but for 1 Jan, and parcels started at 1100 hPa, 655 K and 520 K.

Figure 6. Distribution of parcels initialized on 25 Dec 1993 on the 655 K, 520 K and 420 K isentropic surfaces, plotted on 9 Jan 1994, color coded by their potential temperature (K) on that final day.

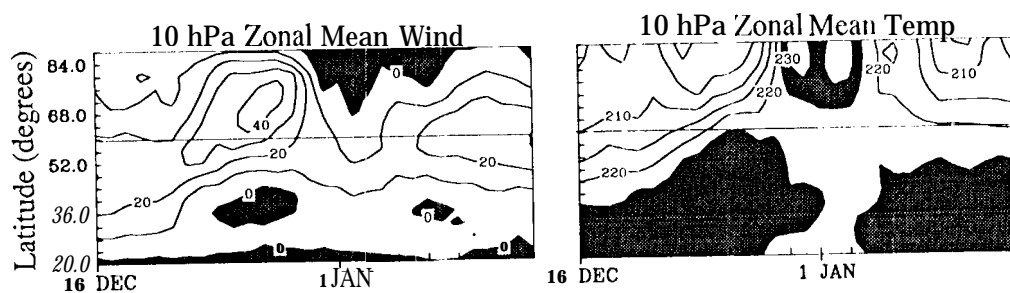


Fig. 1

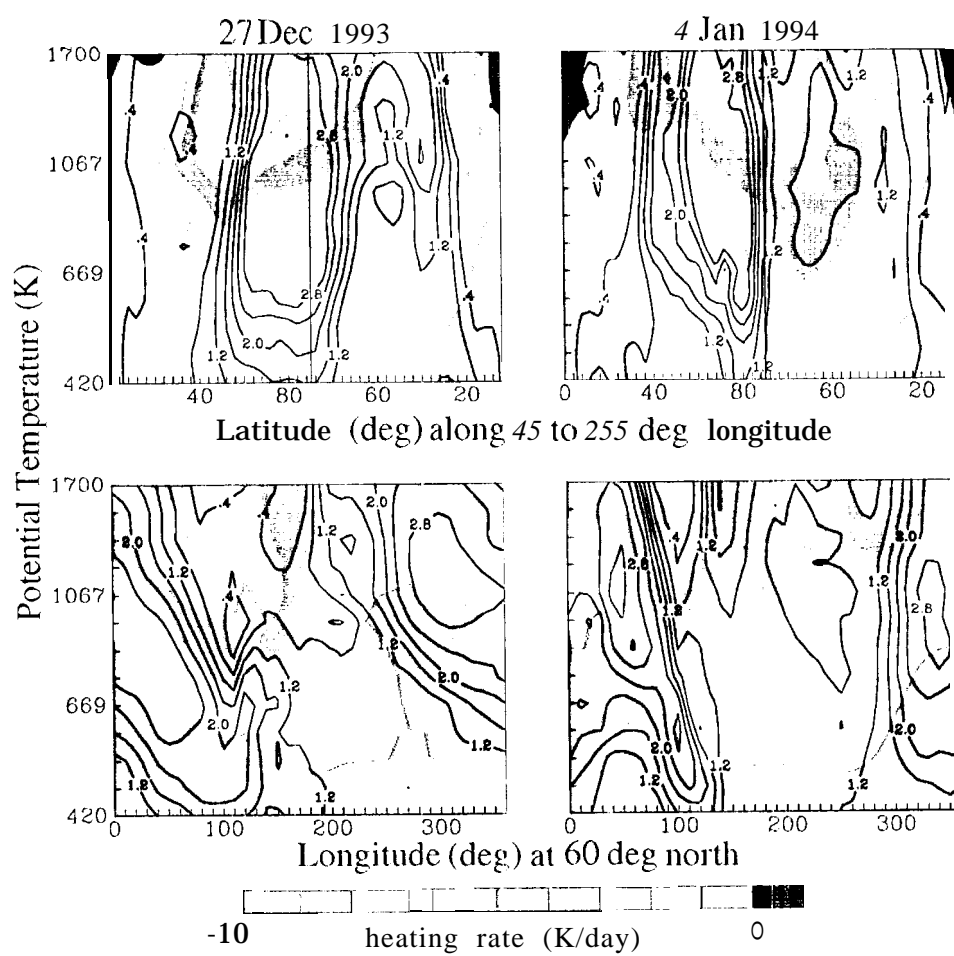


Fig. 2

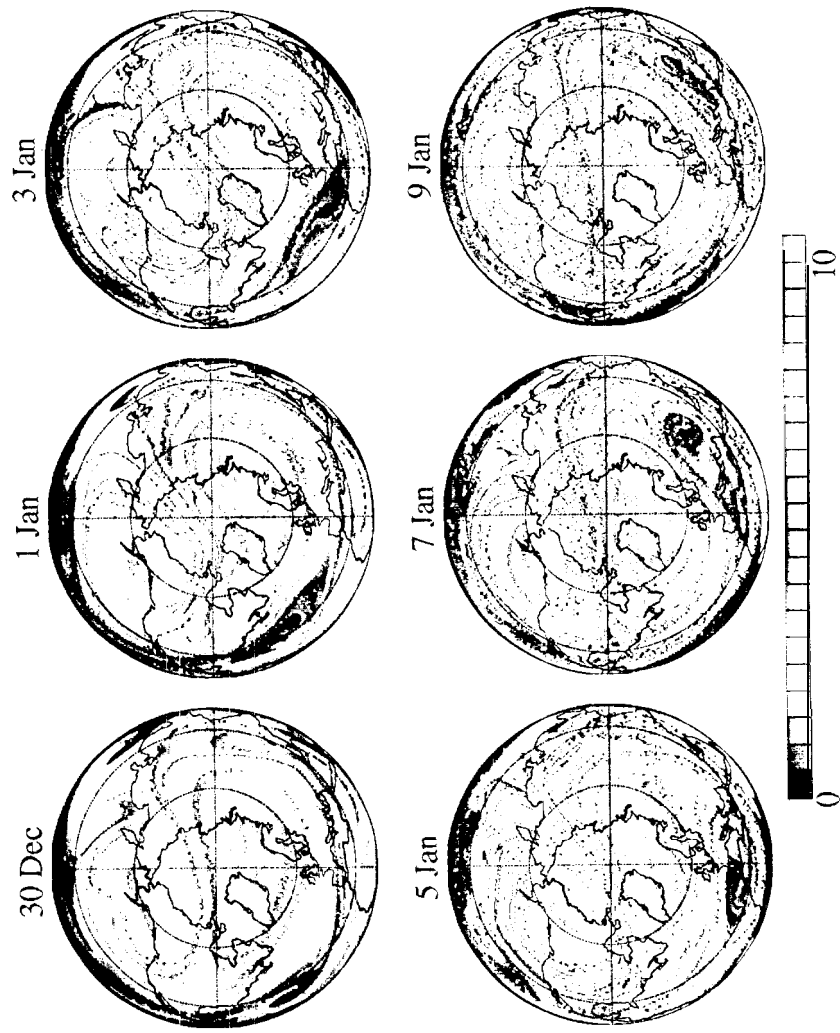


Fig. 3

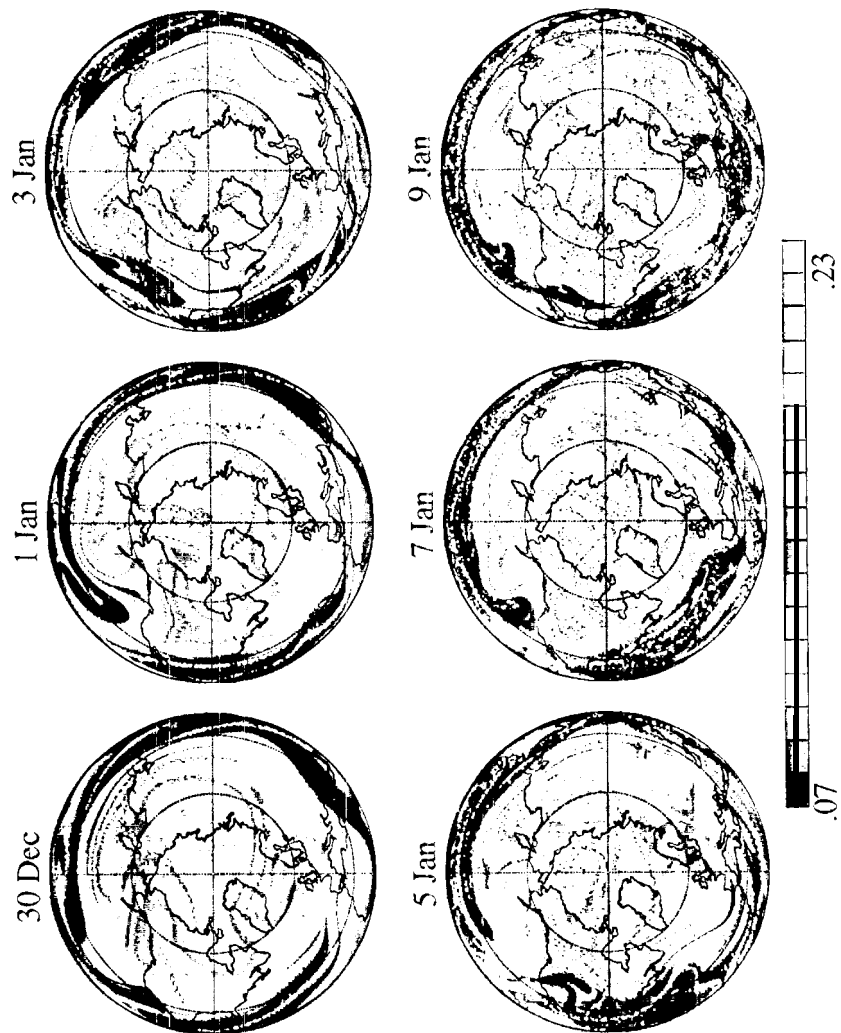


Fig. 4

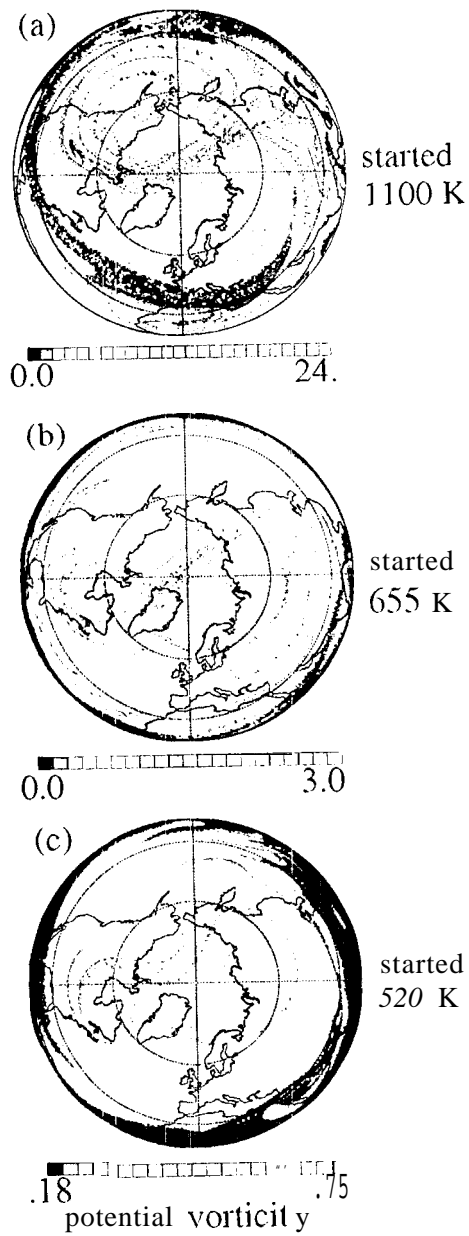


Fig. 5

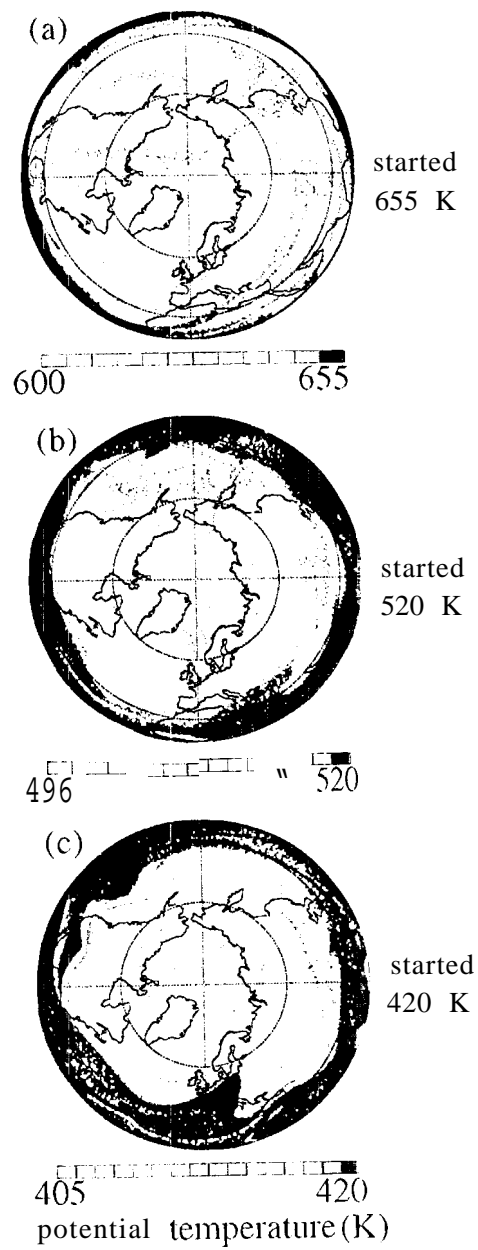


Fig. 6e